

Sodium butyrate inhibits oral squamous cell carcinoma proliferation and invasion by regulating the HDAC1/HSPB7 axis

Hai-Quan YUE¹, Peng-Fei XU², Yi-Dan GUO¹, Jing QI¹, Rui-Min LIU^{1,*}, De-He LI^{3,*}

¹Department of Oral Maxillofacial Surgery, Gansu Provincial Hospital, Lanzhou, Gansu, China; ²Jinchang Integrated Traditional Chinese and Western Medicine Hospital, Jinchang, Gansu, China; ³Department of Stomatology, Jinchang Integrated Traditional Chinese and Western Medicine Hospital, Jinchang, Gansu, China

*Correspondence: lidadehe1988@126.com; liuruimin0909@126.com

Received March 11, 2022 / Accepted May 29, 2022

The study was performed to ascertain the mechanism of sodium butyrate (NaB) mediating the proliferative and invasive properties of oral squamous cell carcinoma (OSCC) cells. The cell proliferative, migrating, and invasive potentials were detected by CCK-8, colony formation, EdU, and Transwell assays. The expression of proliferation- and invasion-related proteins, HDAC1, and HSPB7 in OSCC cells were evaluated by western blot. Immunofluorescence was also performed to evaluate the HDAC1 expression. The enrichment of histone deacetylase HDAC1 in the promoter region of HSPB7 was assessed by the ChIP assay. *In vivo* growth of OSCC cells was measured by tumorigenesis in nude mice (n=18). The t-test was employed for comparisons of data between the two groups. One-way ANOVA was utilized for comparisons of data among multiple groups, and repeated-measures ANOVA for comparisons of data at different time points among groups, followed by Bonferroni post-hoc test. The data showed that HDAC1 expression was highly upregulated in OSCC cells compared to human normal oral keratinocytes (HNOKs) ($p < 0.0001$), and NaB diminished the HDAC1 expression in OSCC cells. NaB restricted OSCC cell proliferative, migrating, and invasive capabilities by downregulating HDAC1. HSPB7 expression was downregulated in OSCC cells versus HNOKs ($p < 0.0001$). HDAC1 inversely orchestrated the HSPB7 expression in OSCC cells through histone deacetylation modification, and NaB augmented the HSPB7 expression by inhibiting HDAC1. Moreover, NaB inhibited OSCC cell growth *in vivo* by elevating HSPB7 levels through the HDAC1 repression. In conclusion, NaB restrained cell proliferation and invasion in OSCC cells via HSPB7 upregulation by decreasing the HDAC1 expression.

Key words: sodium butyrate, histone deacetylase 1, heat shock protein beta-7, oral squamous cell carcinoma, proliferation, invasion

Oral squamous cell carcinoma (OSCC), one of the most frequent malignancies worldwide, is a group of heterogeneous cancers arising from the oral mucosa, which together with oropharyngeal squamous cell carcinoma accounts for more than 90% of oral cancers [1–3]. It usually involves the tongue, lips, gingiva, buccal mucosa, and hard palate and spreads easily to regional lymph nodes and/or distant organs [4]. Consumption of tobacco and alcohol, human papillomavirus infection, dietary and genetic factors, and oral hygiene are risk factors for OSCC [5, 6]. Early diagnosis of OSCC is difficult with most patients being clinically diagnosed at an advanced stage at the initial time of diagnosis [4, 7]. Current OSCC treatment modalities, including EGFR and COX-2 inhibitors, chemical radiation, photodynamic therapy, and tumor resection surgery, lead to major problems associated with non-specific cell death [8]. Furthermore, there is a high

rate of recurrence and metastasis in OSCC patients after treatment, which consequently results in a poor prognosis and a high mortality rate [9]. In this context, there is a strong necessity to determine potential molecular markers affecting cell proliferation and invasion for OSCC diagnosis and prognosis.

A study mentioned that butyrate could inhibit oral cancer cell proliferation [10]. Butyrate reduces ICAM-1 expression in OSCC cells, thereby possibly affecting ICAM-1-dependent migration of leukocytes and immune cells [11]. Sodium butyrate (NaB) is a short-chain fatty acid mainly produced through the fermentation of dietary fiber by gut microbiota [12]. A study indicated that NaB constrained the growth and accelerated apoptosis of head and neck squamous cell carcinoma (HNSCC) cells at millimolar concentrations [13], while one of the highest prevalent malignancies in HNSCC

is OSCC [14]. NaB treatment represses the *in vitro* growth of OSCC cell lines and induces cell cycle arrest [15]. However, the mechanism by which NaB affects OSCC cell growth has not been explored.

The involvement of the family of histone deacetylases (HDACs) has been well documented in tumor progression [16]. Upregulated HDAC2 in pre-cancer and OSCC tissues suggests its implication in the transformation of pre-malignant to malignancy [17]. Silencing of HDAC8 restrains the proliferation of OSCC cells and can activate caspases and autophagy to induce apoptosis of OSCC cells [18]. Overexpression of HDAC9 can promote cell growth and inhibit cell apoptosis in OSCC [19]. Therefore, inhibition of HDACs by HDAC inhibitors constitutes a novel and highly selective family of anticancer agents and exhibits remarkable antitumor activity in some human malignancies, including OSCC [16]. NaB, an HDAC inhibitor, suppresses deacetylase activity, and NaB has been shown to inhibit HDAC1 expression [20, 21]. Hence, we speculated that NaB might influence the progression of OSCC through HDAC1.

The binding sites between HDAC1 and the heat shock protein beta-7 (HSPB7) promoter region were predicted through the bioinformatics website UCSC. The tumor suppressor HSPB7 was reported to be inactivated in malignant tumors [2], including renal cell carcinomas [22]. Therefore, we hypothesized that NaB might influence OSCC progression by regulating HDAC1 and thus modulating HSPB7 expression. This study was designed to confirm this hypothesis.

Materials and methods

Cell culture and cell grouping. Human OSCC cell lines SCC-15 and CAL-27 were bought from the American Type Culture Collection. Human normal oral keratinocytes (HNOKs) from three healthy volunteers were isolated and used as normal controls. SCC-15 and CAL-27 cells were cultured in Dulbecco's modified Eagles medium (DMEM)-F12 encompassing 10% fetal bovine serum [23]. HNOKs were cultured in an oral keratinocyte medium with 1% oral keratinocyte growth supplement, 100 U/ml penicillin, and 0.1 mg/ml streptomycin in constant temperature incubators (37°C, 5% CO₂) [24].

Lentivirus plasmid harboring overexpression (oe)-HDAC1, oe-negative control (NC), short hairpin RNA (sh)-HSPB7, and sh-NC and viral packaging kits were obtained from GeneCopoeia. After lentivirus transfection reagents were co-transfected into HEK293T for 48 h, a p24 ELISA kit was employed to measure the viral titer in each group. The viral titer for the sh-HSPB7 and oe-HDAC1 groups was 5×10^8 TU/ml and that for the control group was 8×10^8 TU/ml. Subsequently, OSCC cells were infected for 24 h with the obtained lentiviral particles, and then cultured for 48 h. Stably infected cell lines were screened by puromycin because vectors containing a puromycin-resistant gene were

used and then the infection efficiency was assessed by quantitative real-time polymerase chain reaction (qRT-PCR) [25, 26]. The cells were treated with NaB (5 mM) for 24 h. NaB was purchased from Sigma.

Cell counting kit (CCK)-8. Cell viability was detected using a CCK-8 kit [27]. SCC-15 and CAL-27 cells at the logarithmic growth stage were pre-cultured in 96-well plates at 1×10^4 cells/well for 24 h. Then the cells were transfected based on the grouping. After 48 h of transfection, cells were incubated with 10 μ l CCK-8 reagent at 37°C for 3 h. The absorbance value of each well at 450 nm was measured on a microplate reader.

Colony formation assay. Agar with a concentration of 1.2% was dissolved by heating and set aside in a water bath at 46°C. The prepared SCC-15 and CAL-27 cells were counted and suspended in DMEM preheated at 40°C. A volume of 325 μ l of cell suspension was added into each well of a 24-well culture plate, and added and mixed with 50 μ l of the sample. Spare agar (125 μ l) was aspirated and rapidly mixed with the above mixture in a 24-well plate, avoiding any air bubbles. After natural solidification, the 24-well plates underwent 14-day incubation at 37°C with 5% CO₂. Subsequently, cells were subjected to fixing with 10% formaldehyde, 15 min staining with 0.1% crystal violet, and observation under an inverted microscope [28].

5-ethynyl-2'-deoxyuridine (EdU) assay. Referring to the method in previous research [29] and EdU instructions, cells were seeded into 24-well plates with 3 replicate wells for each group of cells. EdU reagents were added to the culture medium for a concentration of 10 μ mol/l. After 2 h of incubation, the medium was removed. Cells were fixed with phosphate-buffered saline (PBS) solution containing 4% paraformaldehyde for 15 min at room temperature and washed with PBS containing 3% bovine serum albumin (BSA) twice. Cells were then incubated with 0.5% Triton-100 PBS for 20 min at room temperature and washed with PBS containing 3% BSA twice. After 100 μ l Apollo® 567 was added to each well, cells were incubated for 30 min at room temperature protected from light, and washed with PBS containing 3% BSA twice. Then 4',6-diamidino-2-phenylindole (DAPI) was added to stain the nucleus for 5 min, and PBS was applied to rinse the cells three times. After the slides were sealed, the positive cell counts within each area were examined under a fluorescence microscope. Under the microscope, the total cells were in blue and the positive cells were in red, and five fields of view were selected randomly in each well to calculate the proportion of positive cells for EdU staining. EdU positive rate = (number of EdU positive nucleus/total nucleus) \times 100% [30].

Transwell assay. OSCC cells were starved in a serum-free medium for 24 h and digested and the cell density was adjusted to 3×10^4 cells/ml. Experiments were performed using 24-well plates in 8 μ m Transwell chambers with or without 50 μ l Matrigel matrix gel in the chambers. Each group had 3 chambers. Each chamber was added with cell

suspension (100 μ l) with 500 μ l of 10% DMEM added to each lower chamber and incubated at 37 °C with 5% CO₂ for 24 h. Then, cells were fixed with 4% paraformaldehyde for 30 min before 0.1% crystal violet staining for 30 min. The stained cell numbers were counted under the inverted microscope. Five fields were randomly selected for counting [31]. Three experiments were repeated.

Western blot (WB). Tissues or cells were collected by trypsin digestion and lysed with enhanced radio-immunoprecipitation assay lysis solution containing protease inhibitors, and then protein concentrations were determined with a bicinchoninic acid protein quantification kit. Proteins were separated by 10% sodium dodecyl sulfate-polyacrylamide gel electrophoresis, transferred to polyvinylidene fluoride membranes, and blocked in 5% BSA at room temperature for 2 h to block nonspecific binding. Then, the proteins were incubated with diluted primary antibodies against HDAC1 (ab280198, 1:1000, Abcam), HSPB7 (ab150390, 1:2000, Abcam), proliferating cell nuclear antigen (PCNA, ab92552, 1:2500, Abcam), matrix metalloproteinase 2 (MMP2, ab92536, 1:2500, Abcam), MMP9 (ab76003, 1:2000, Abcam), and glyceraldehyde-3-phosphate dehydrogenase (GAPDH, ab9485, 1:2500, Abcam) overnight at 4 °C, respectively. After the membranes were washed, HRP-labeled goat anti-rabbit secondary antibody (ab6721, 1:2000, Abcam) was added for incubation at room temperature for 1 h. The membranes were incubated with electrogenerated chemiluminescence (ECL) working solution for 1 min at room temperature, and then the excess ECL solution was removed. The membranes were sealed with cling film and developed and fixed after 5–10 min exposure to X-ray film in the dark box. The bands were quantified in gray-scale using ImageJ analysis software and GAPDH was used as the internal reference [30]. Three experiments were repeated.

Immunofluorescence. Referring to the methodology of literature [32] with some modifications, the slides were fixed for 15 min with 4% paraformaldehyde. The slides were washed 3 times with PBS and then dried with absorbent paper. Normal goat serum was applied to the slides to block the unspecific reaction for 30 min. Then, the blocking solution was removed with absorbent paper without washing, and each slide was incubated with primary antibodies against HDAC1 (ab109411, 1:50, Abcam) overnight at 4 °C. The slides were washed with phosphate-buffered saline with Tween 20 three times for 3 min each and incubated for 1 h at 37 °C protected from light with Alexa Fluor 488-labeled goat anti-rabbit immunoglobulin G (ab150077, Abcam) (fluorescence in green). After being washed with PBS 3 times in the dark, the slides were stained for 5 min with 5 μ g/ml DAPI and then washed with PBS for 5 min, 3 times. The slides were stored at 4 °C away from light and the results were observed and pictured by NIS-Elements Viewer software using a laser scanning confocal microscope.

Chromatin immunoprecipitation (ChIP) assay. According to the method previously described [33], after

treatment with 4% formaldehyde (the final concentration of formaldehyde was 1%), the collected SCC-15 and CAL-27 cells were subjected to ultrasonication. Primary antibodies against HDAC1 (ab280198, 1:50, Abcam) were added to bind to the HSPB7 gene promoter. Protein A Agarose/Salmon Sperm DNA was added to bind to the gene promoter complex, followed by precipitation of the complex. The precipitated complex was washed to remove non-specific bindings. After elution, the complex with enrichment of HSPB7 gene promoter was de-crosslinked and purified, followed by qPCR. HSPB7 promoter primers were detailed as follows: forward, 5'-CATAGGCCAGTGATGAAGCC-3'; reverse, 5'-GCTCTGCTGACCCTAACTCTT-3'.

Subcutaneous tumorigenesis experiment in nude mice. Referring to the previously reported methods [34, 35], eighteen SPF-grade male BALB/c nude mice (5 weeks, 15–18g) were randomly assigned into three groups: control+sh-NC group, NaB+sh-NC group, and NaB+sh-HSPB7 group, with six mice in each group. SCC-15 cell suspension at a concentration of about 1×10^7 cells/ml was injected into the skin of the left axilla of nude mice with a 1 ml syringe to establish a nude mouse subcutaneous transplantation tumor model. After the tumor reached a certain volume, the BALB/c nude mice were executed by the cervical dislocation method on day 28 (the execution method was in accordance with the ethical statement). The tumor tissues were peeled out, photographed, and weighed and the tumor size was calculated [36]. Animal use and experimental procedures during the experiments complied with animal ethics standards and the animal experiments were all reviewed and approved by the Animal Experimentation Ethics Committee of Jinchang Integrated Traditional Chinese and Western Medicine Hospital.

Statistical analysis. SPSS version 19.0 was conducted for statistical analysis. The measurement data were represented as mean \pm SD, t-test was employed to compare between two groups, one-way ANOVA was used for comparison of data among multiple groups, and repeated-measures ANOVA was used for comparison of data among groups at different time points, and Bonferroni was used for post hoc tests. A p-value <0.05 indicates that the difference is statistically significant.

Results

NaB inhibited OSCC cell proliferation and invasion. To investigate the effect of NaB on the cell proliferation and invasion of OSCC, OSCC cells were treated with NaB. With respect to CCK-8 assays, SCC-15 and CAL-27 cell viability in the NaB group was remarkably declined compared with the control group (Figure 1A, $p < 0.05$). The clone formation assay demonstrated that SCC-15 and CAL-27 cell clone formation ability was prominently decreased in the NaB group versus the control group (Figure 1B, $p < 0.05$). Also, EdU assay results exhibited that SCC-15 and CAL-27 cell proliferation was dramatically lower in the NaB group than in the

control group (Figure 1C, $p < 0.05$). The results of Transwell assay exhibited that SCC-15 and CAL-27 cell migration and invasion were notably diminished in the NaB group rather than in the control group (Figures 1D, 1E; $p < 0.05$). WB results displayed that the expression of proliferation- and invasion-related proteins PCNA, MMP2, and MMP9 was substantially reduced in the NaB group in comparison to the

control group (Figure 1F, $p < 0.05$). The above results indicated that NaB inhibited cell proliferation and invasion in OSCC.

NaB restrained HDAC1 expression in OSCC cells. starBase predicted the elevated HDAC1 expression in oral cancer-associated cancers (Figure 2A), which was in line with the previous study [37]. Therefore, we investigated whether NaB influenced OSCC progression by regulating

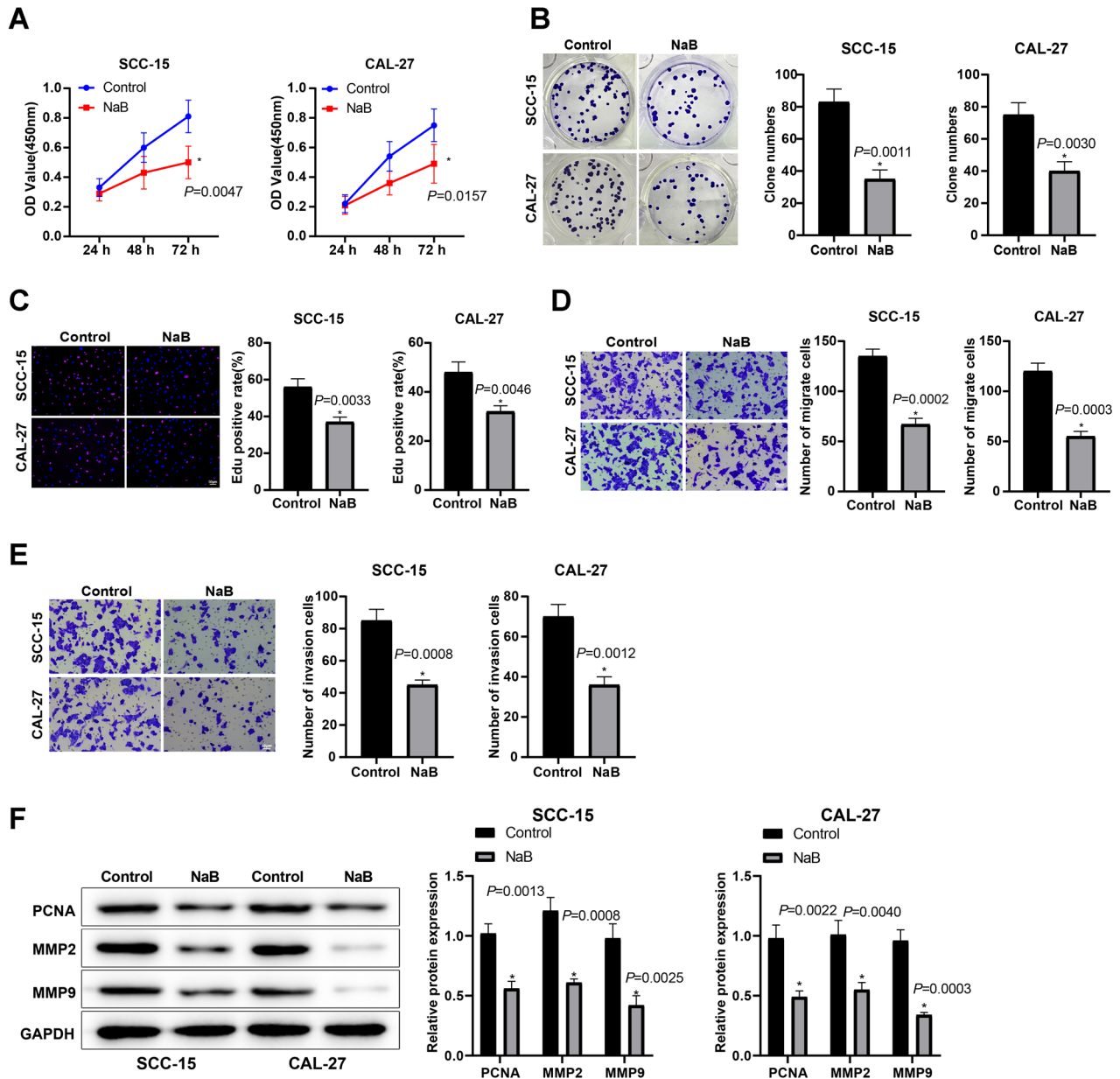


Figure 1. NaB restrains OSCC cell proliferation and invasion. A–C) SCC-15 and CAL-27 cell proliferation was detected by CCK-8 (A), clone formation (B), and EdU (C, $\times 200$) assays; D, E) SCC-15 and CAL-27 cell migration (D) and invasion (E) were evaluated by Transwell assay ($\times 200$); F) Expression of proliferation- and invasion-related proteins PCNA, MMP2, and MMP9 in SCC-15 and CAL-27 cells was assessed by western blot; * indicates compared with the control group, $p < 0.05$; values in the figures were measurement data, which were expressed as mean \pm standard deviation. An independent sample t-test was used for pairwise comparisons, and repeated measurement analysis of variance was utilized for comparisons of data among groups at different time points, with Bonferroni for post hoc tests. The experiment was repeated three times. Abbreviations: NaB-sodium butyrate; OSCC-oral squamous cell carcinoma; PCNA-proliferating cell nuclear antigen; MMP2-matrix metalloproteinase 2

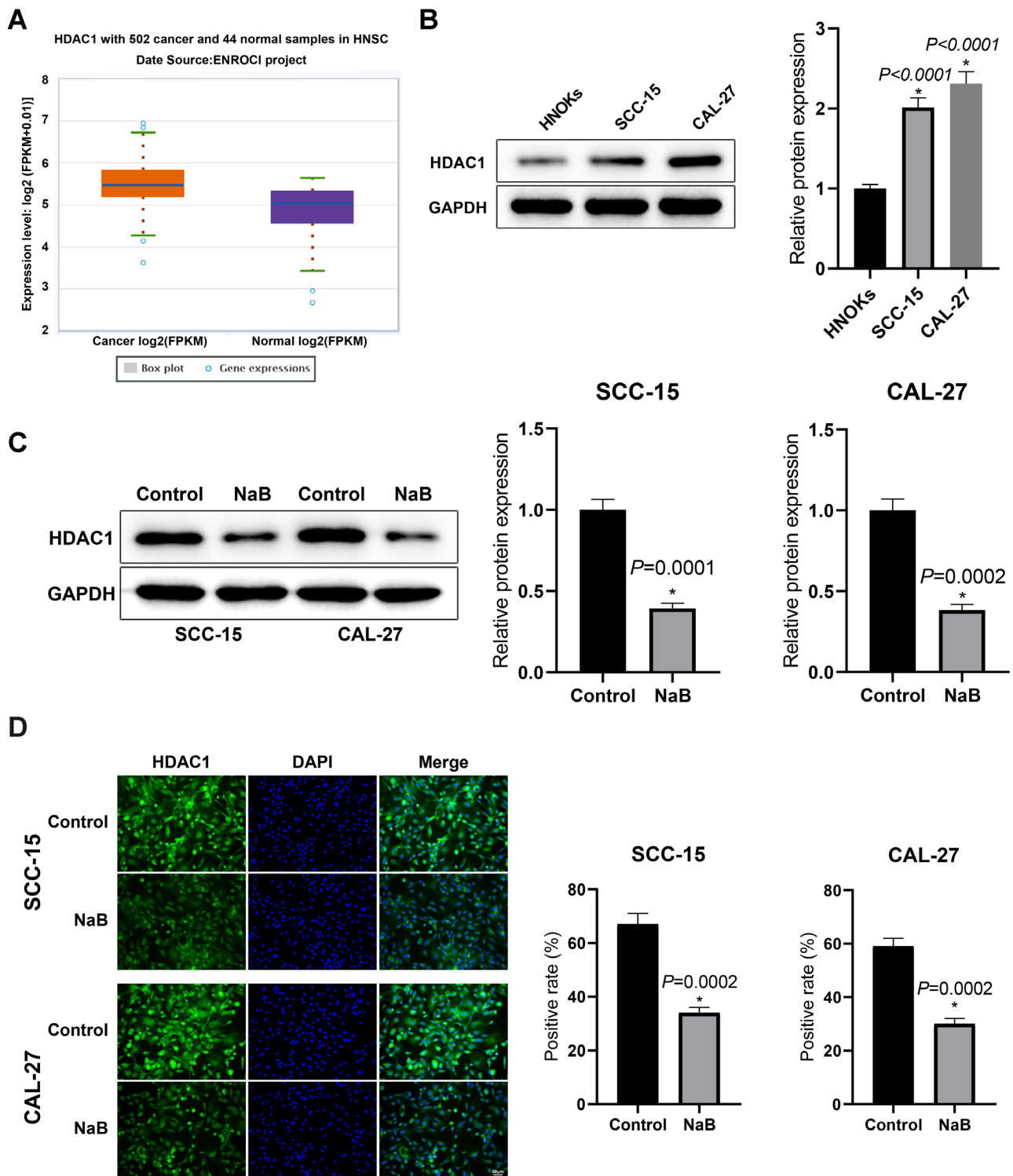


Figure 2. NaB curbs HDAC1 expression in OSCC. A) Bioinformatics predicted that HDAC1 was highly expressed in head and neck squamous cell carcinoma; B) HDAC1 expression was tested in HNOks, SCC-15, and CAL-27 cells by western blot; C) HDAC1 expression was determined in SCC-15 and CAL-27 cells after NaB treatment by western blot; D) HDAC1 positive rate was examined in SCC-15 and CAL-27 cells after NaB treatment by immunofluorescence ($\times 200$); *indicates compared with the normal group, the HNOks group, or the control group, $p < 0.05$; values in the figures were measurement data, which were expressed as mean \pm standard deviation. An independent sample t-test was used for pairwise comparison, and the experiment was repeated three times. Abbreviations: NaB-sodium butyrate; HDAC1-histone deacetylase 1; OSCC-oral squamous cell carcinoma; HNOks-human normal oral keratinocytes

HDAC1 expression. WB data demonstrated that HDAC1 expression was obviously enhanced in the SCC-15 and CAL-27 cells compared with HNOKs (Figure 2B, $p < 0.05$). Moreover, HDAC1 expression was remarkably declined in the NaB group versus the control group (Figure 2C, $p < 0.05$). Immunofluorescence also showed that the positive rate of

HDAC1 in the NaB group was strikingly lower than that of the control group (Figure 2D, $p < 0.05$). Taken together, NaB repressed HDAC1 expression in OSCC cells.

NaB suppressed the proliferation and invasion of OSCC cells by downregulating HDAC1. To investigate whether NaB affects OSCC by mediating HDAC1 expression, HDAC1

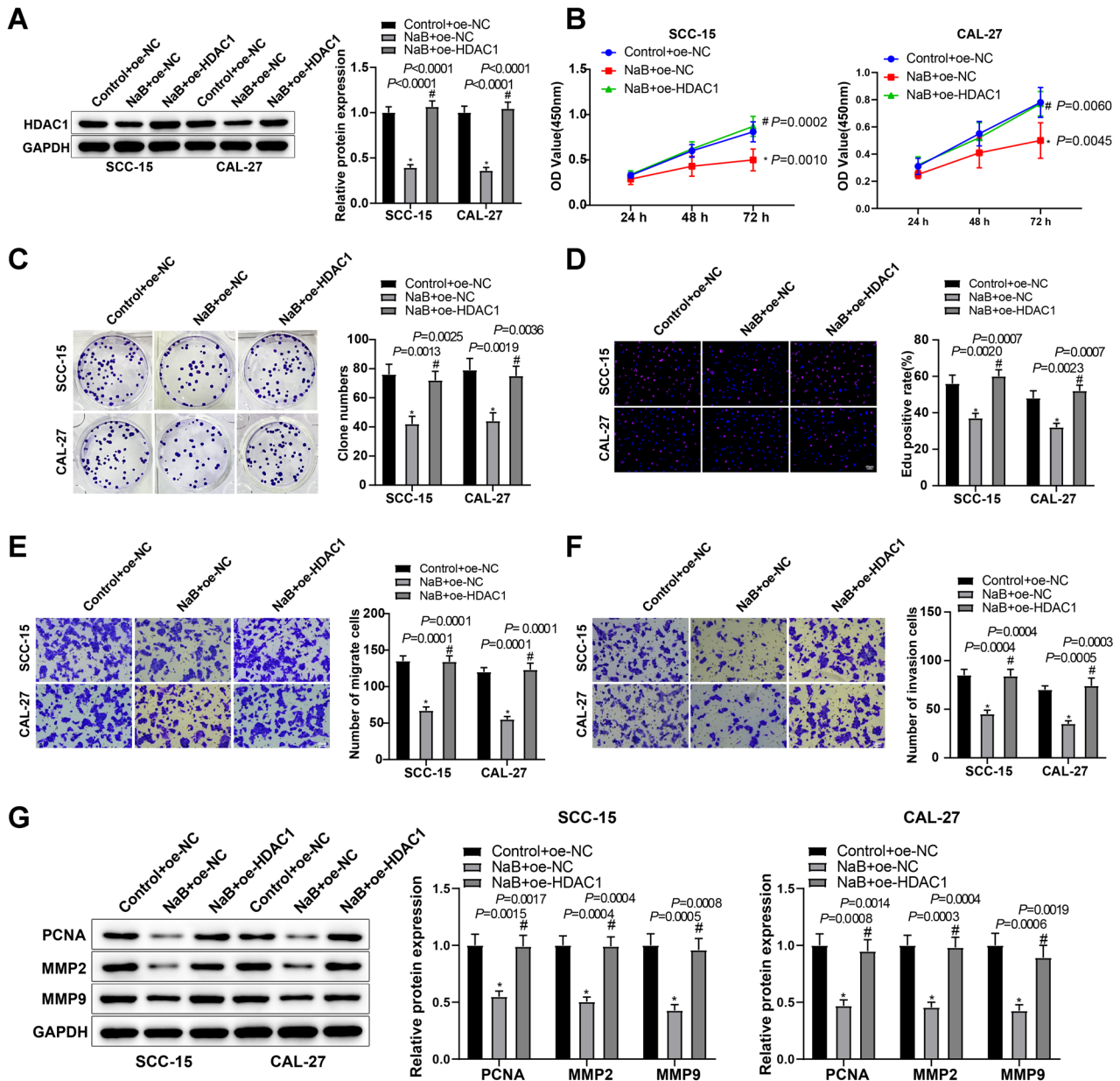


Figure 3. NaB constrains OSCC cell proliferation and invasion by downregulating HDAC1. A) HDAC1 expression in SCC-15 and CAL-27 cells was detected by western blot; B–D) SCC-15 and CAL-27 cell proliferation was evaluated by CCK-8 (B), clone formation (C), and EdU (D, $\times 200$) assays; E, F) SCC-15 and CAL-27 cell migration (E) and invasion (F) were measured by Transwell assay ($\times 200$); G) Expression of PCNA, MMP2, and MMP9 in SCC-15 and CAL-27 cells was examined by western blot; * indicates compared with the control+oe-NC group, $p < 0.05$; # indicates compared with the NaB+oe-NC group, $p < 0.05$; values in the figures were measurement data, which were expressed as mean \pm standard deviation. Data comparison among multiple groups was conducted using one-way analysis of variance, and data comparison among groups at different time points was performed using repeated-measures analysis of variance, with post hoc tests using Bonferroni. The experiment was repeated three times. Abbreviations: NaB-sodium butyrate; OSCC-oral squamous cell carcinoma; HDAC1-histone deacetylase 1; PCNA-proliferating cell nuclear antigen; MMP2-matrix metalloproteinase 2

expression was detected in SCC-15 and CAL-27 cells, which were treated with oe-HDAC1 and NaB. The results manifested that HDAC1 expression was remarkably reduced in the NaB+oe-NC group compared with the control+oe-NC group but obviously enhanced in the NaB+oe-HDAC1 group compared with the NaB+oe-NC group (Figure 3A, $p < 0.05$). As reflected by the results of CCK-8, clone formation, and EdU assays, SCC-15 and CAL-27 cell proliferation and clone formation were conspicuously diminished in the NaB+oe-NC group relative to the control+oe-NC group but prominently elevated in the NaB+oe-HDAC1 group in contrast to the NaB+oe-NC group (Figures 3B–3D; $p < 0.05$). Transwell assay depicted that SCC-15 and CAL-27 cell migrating and invasive abilities in the NaB+oe-NC group were appreciably decreased in comparison to the control+oe-NC group, while the opposite trends were observed in the NaB+oe-HDAC1 group versus the NaB+oe-NC group (Figures 3E, 3F; $p < 0.05$). The NaB+oe-NC group had observable declines in PCNA, MMP2, and MMP9 expression compared with the control+oe-NC group, which was contrary to the NaB+oe-HDAC1 group relative to the NaB+oe-NC group (Figure 3G, $p < 0.05$). In conclusion, NaB curbed cell proliferation and invasion in OSCC by suppressing HDAC1.

HDAC1 curtailed HSPB7 expression through histone deacetylation in OSCC cells. The bioinformatics website UCSC predicted the histone acetylase binding sites in the HSPB7 promoter region (Figure 4A), while bioinformatics database analysis manifested that HSPB7 was lowly expressed in HNSCC (Figure 4B). WB indicated that HSPB7 expression was remarkably decreased in SCC-15 and CAL-27 cells compared with the HNOKs (Figure 4C, $p < 0.05$), revealing that HSPB7 was lowly expressed in OSCC. The binding of HDAC1 to the HSPB7 promoter region was verified by ChIP assay, which showed that HDAC1 enrichment in the HSPB7 promoter region was considerably augmented in SCC-15 and CAL-27 cells versus HNOKs (Figure 4D, $p < 0.05$). After silencing of HDAC1 in SCC-15 and CAL-27 cells, HDAC1 enrichment in the HSPB7 promoter region was evidently diminished in the sh-HDAC1 group versus the sh-NC group (Figure 4E, $p < 0.05$). WB indicated that HDAC1 expression was remarkably reduced and HSPB7 expression was obviously enhanced in the sh-HDAC1 group compared with the sh-NC group (Figure 4F, $p < 0.05$). Also, the same trends were shown in the NaB group relative to the control group (Figure 4F, $p < 0.05$). Collectively, HDAC1 restrained HSPB7 expression through histone deacetylation in OSCC cells, while NaB promoted HSPB7 expression through inhibition of HDAC1.

NaB restricted cell proliferation and invasion in OSCC via the HDAC1/HSPB7 axis. To investigate whether NaB affected OSCC through the HDAC1/HSPB7 axis, SCC-15 and CAL-27 cells were transfected with sh-HSPB7 and treated with NaB. As discovered by WB results, there existed noticeably reduced HSPB7 expression in the NaB+sh-HSPB7 group compared with the NaB+sh-NC group (Figure 5A, $p < 0.05$). CCK-8, EdU, and clone formation assays exhibited

that SCC-15 and CAL-27 cell proliferation and clone formation were obviously enhanced in the NaB+sh-HSPB7 group versus the NaB+sh-NC group (Figures 5B–5D; $p < 0.05$). With regard to Transwell assay results, SCC-15 and CAL-27 cell migrating and invasive abilities in the NaB+sh-HSPB7 group were noticeably elevated in contrast to the NaB+sh-NC group (Figures 5E, 5F; $p < 0.05$). WB results demonstrated that the expression of PCNA, MMP2, and MMP9 was markedly augmented in the NaB+sh-HSPB7 group in comparison to the NaB+sh-NC group (Figure 5G, $p < 0.05$). In conclusion, NaB inhibited proliferation and invasion of OSCC cells by promoting HSPB7 expression through HDAC1 downregulation.

NaB retarded OSCC growth *in vivo* via the HDAC1/HSPB7 axis. To verify the effect of NaB on OSCC *in vivo*, we performed tumorigenic experiments in nude mice. The measurement of tumor growth and volume demonstrated that the tumor growth, tumor volume, and weight were prominently diminished in the NaB+sh-NC group compared with the control+sh-NC group but substantially enhanced in the NaB+sh-HSPB7 group versus the NaB+sh-NC group (Figures 6A–6C, $p < 0.05$). As depicted by WB results, the NaB+sh-NC group exhibited conspicuously diminished HDAC1 expression and considerably augmented HSPB7 expression versus the control+sh-NC group (Figure 6D, $p < 0.05$). Conversely, HSPB7 expression was noticeably reduced in the NaB + sh-HSPB7 group in contrast to the NaB+sh-NC group (Figure 6D, $p < 0.05$). Overall, NaB subdued OSCC cell growth *in vivo* by upregulating HDAC1-modulated HSPB7.

Discussion

As one of the highly prevalent head and neck cancers, OSCC is the primary reason for morbidity and mortality in head and neck cancer patients [8]. In spite of tremendous improvement in treatment, the five-year overall survival of OSCC has remained constant over the last few decades [38]. Thus, the research of novel approaches is a necessity for the treatment of OSCC. Through cell and nude mice experiments, this study revealed that NaB repressed OSCC proliferation and invasion through upregulation of HSPB7 via suppression of HDAC1.

Many studies have demonstrated that NaB could inhibit tumor cell propagation, differentiation, and apoptosis in various tissues, such as the colon and stomach [39, 40]. A study displayed that NaB reduced the invasiveness of OSCC-derived cells by promoting dermatopontin expression [41]. NaB restricts invasion and metastasis by inhibiting Podoplanin expression in oral and pharyngeal squamous cell carcinoma cell lines [42]. NaB could subdue the growth and induce cell cycle G1 arrest in OSCC cell lines [43]. Similar to the above literature results, our experimental results depicted that NaB curtailed cell proliferation and invasion in OSCC, but the exact mechanism remains to be verified.

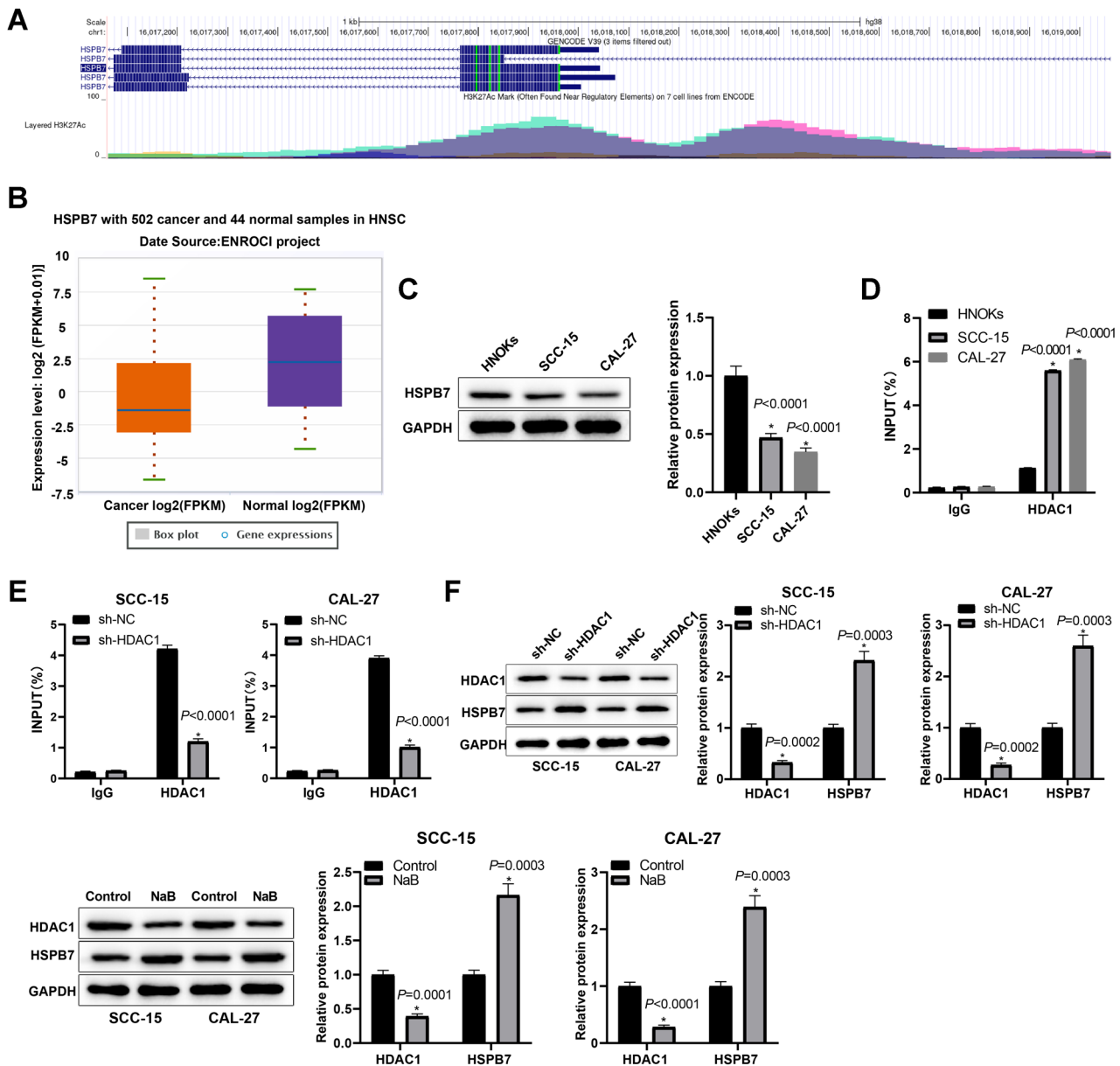


Figure 4. HDAC1 suppresses HSPB7 expression in OSCC cells. **A)** Bioinformatics website UCSC predicted the histone acetylase binding sites in the HSPB7 promoter region; **B)** Bioinformatics database analyzed HSPB7 expression in head and neck squamous cell carcinoma; **C)** HSPB7 expression in SCC-15 and CAL-27 cells was detected by western blot; **D)** The binding of HDAC1 to the HSPB7 promoter region was evaluated by ChIP assay; **E)** The binding of HDAC1 to the HSPB7 promoter region after silencing HDAC1 was assessed by ChIP assay; **F)** HDAC1 and HSPB7 expression was measured by western blot; *indicates compared with the normal group, the HNOKs group, the sh-NC group, or the control group, $p < 0.05$; values in the figures were measurement data, which were expressed as mean \pm standard deviation. An independent sample t-test was used for pairwise comparison, and the experiment was repeated three times. Abbreviations: NaB-sodium butyrate; OSCC-oral squamous cell carcinoma; HDAC1-histone deacetylase 1; HSPB7-heat shock protein beta-7; HNOKs-human normal oral keratinocytes

In tongue squamous carcinoma cells, HDAC1 overexpression was shown to be substantially associated with lymph node metastasis [44]. miR-874 inhibited HNSCC cell proliferation through direct targeting of HDAC1 [45]. HDAC1 was also demonstrated to accelerate OSCC growth and progression by regulating miR-154-5p/PCNA signaling

[37]. The inhibitors of histone deacetylation, as well as NaB, were already proposed to be utilized as anticancer agents for rapidly growing tumors that appear to be highly resistant to chemotherapy [46]. NaB was described to inhibit the expression of HDAC1 and 3 [20]. Consistent with the previous studies, our results elaborated that NaB retarded the

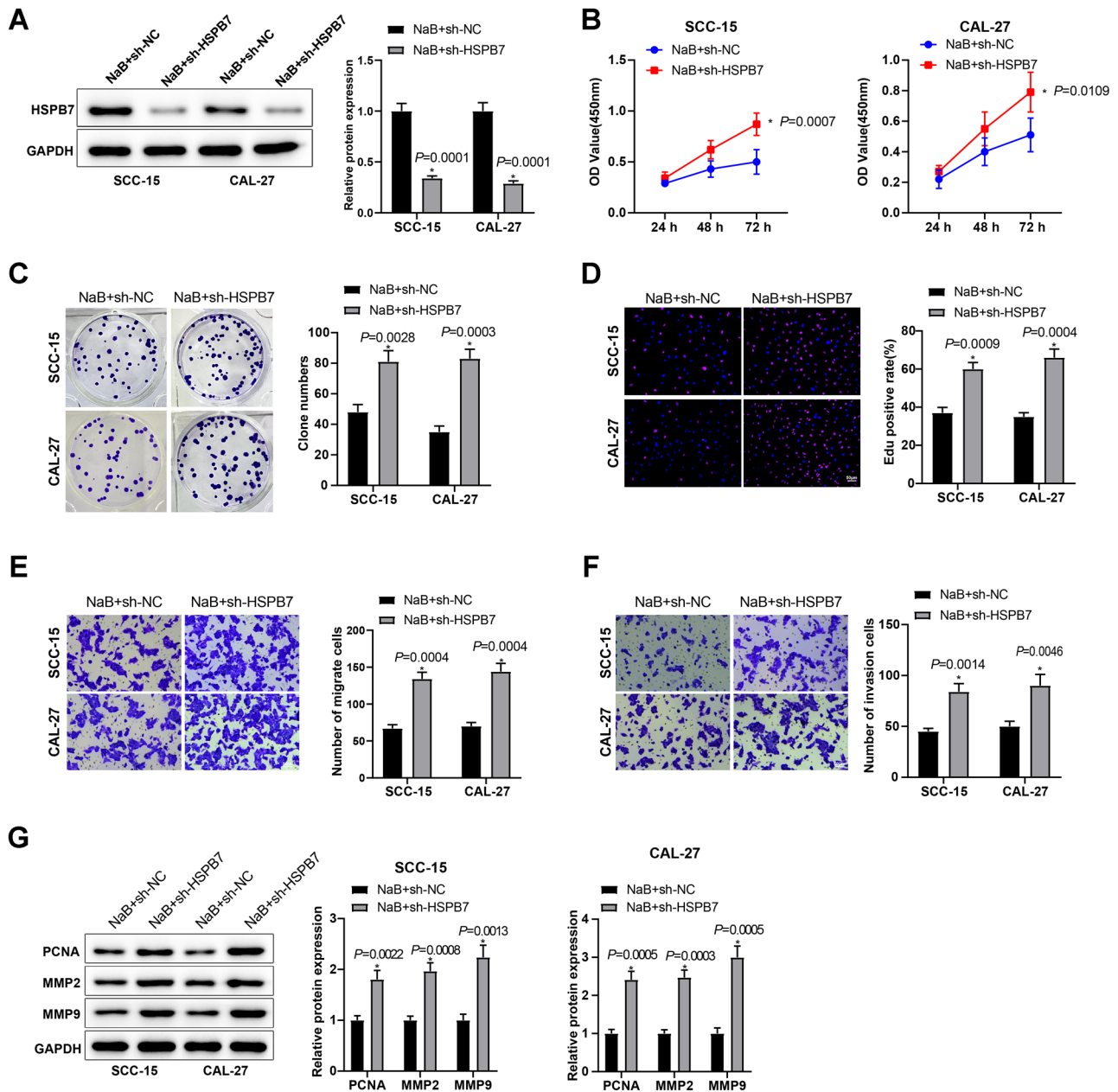


Figure 5. NaB curtails OSCC cell proliferation and invasion by manipulating the HDAC1/HSPB7 axis. **A**) HSPB7 expression in SCC-15 and CAL-27 cells was detected by western blot; **B–D**) SCC-15 and CAL-27 cell proliferation was assessed by CCK-8 (**B**), clone formation (**C**), and EdU (**D**, $\times 200$) assays; **E, F**) SCC-15 and CAL-27 cell migration (**E**) and invasion (**F**) were determined by Transwell assay ($\times 200$); **G**) Expression of PCNA, MMP2, and MMP9 in SCC-15 and CAL-27 cells was evaluated by western blot; *indicates compared with the NaB+sh-NC group, $p < 0.05$; values in the figures were measurement data, which were expressed as mean \pm standard deviation. Independent sample t-test was used for pairwise comparison, and repeated measurement analysis of variance was employed for comparisons of data among groups at different time points, with Bonferroni for post hoc tests. The experiment was repeated three times. Abbreviations: NaB-sodium butyrate; OSCC-oral squamous cell carcinoma; HDAC1-histone deacetylase 1; HSPB7-heat shock protein beta-7; PCNA-proliferating cell nuclear antigen; MMP2-matrix metalloproteinase 2

expression of HDAC1 in OSCC cells. Moreover, our experimental data uncovered that HDAC1 upregulation nullified the repressive influence of NaB on OSCC cell proliferation and invasion. Next, we investigated the downstream targets of HDAC1 that are potentially involved in the OSCC process.

HSPB7 is a member of the small heat shock protein family with crucial roles in the maintenance of cellular homeostasis in multiple both physiological and pathophysiological processes [47]. Bioinformatics database analysis presented that HSPB7 was lowly expressed in HNSCC. Similar to a

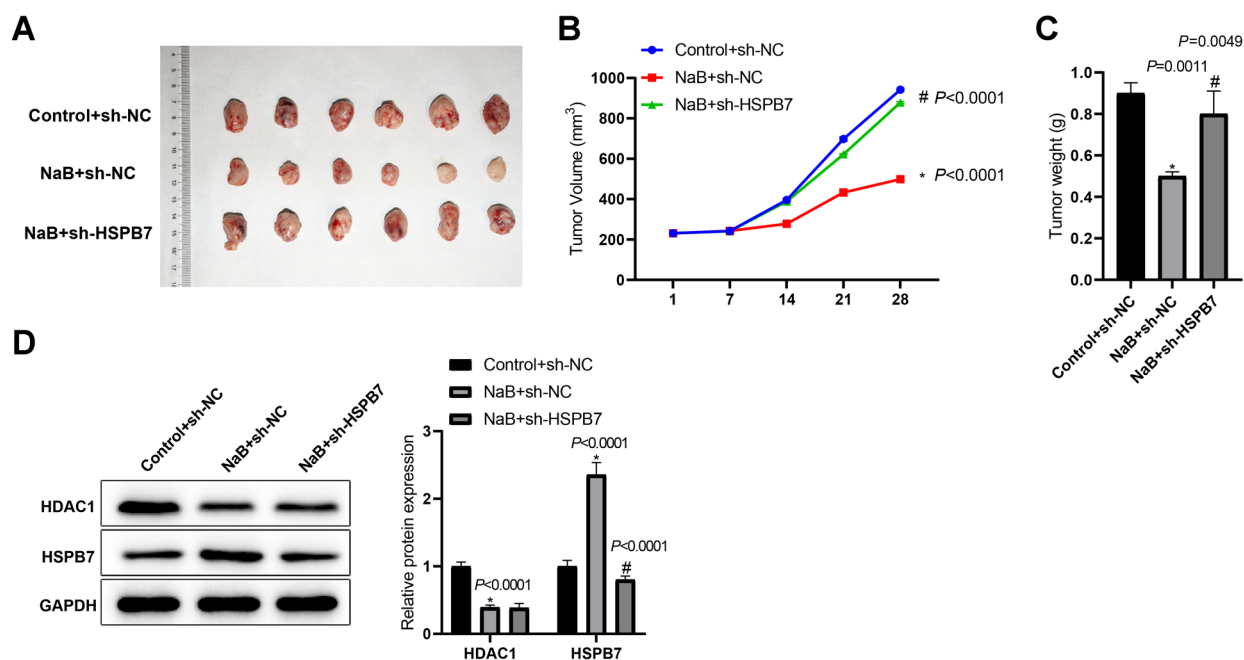


Figure 6. NaB represses OSCC growth *in vivo* via the HDAC1/HSPB7 axis. A) Representative images of tumors extracted from nude mice; B) Tumor volume growth curve from day 1 to day 28; C) Tumor weight; D) HDAC1 and HSPB7 expression in tumor tissues was detected by western blot; data were expressed as mean \pm standard deviation, and one-way analysis of variance was used to compare data among multiple groups, followed by Tukey's post hoc tests. Data among groups at different time points were compared using repeated-measures analysis of variance with Bonferroni for post hoc tests. *indicates compared with the control+sh-NC group, $p < 0.05$; #indicates compared with the NaB+sh-NC group, $p < 0.05$, $N = 6$. Abbreviations: NaB-sodium butyrate; OSCC-oral squamous cell carcinoma; HDAC1-histone deacetylase 1; HSPB7-heat shock protein beta-7

previous study [2], our study exhibited a low HSPB7 expression in OSCC cells. Meanwhile, the bioinformatics site UCSC predicted the binding sites for histone acetylase in the HSPB7 promoter region. However, the relationship between HDAC1 and HSPB7 has never been reported. Of note, our results elucidated that HDAC1 restricted HSPB7 expression through histone deacetylation modification and that NaB elevated HSPB7 expression by inhibiting HDAC1. Lin et al. possessed that HSPB7 is a potential anti-cancer gene for renal cell carcinoma, which curbs the cell growth in renal cell carcinoma [22]. Similarly, our experiments uncovered that silencing HSPB7 abrogated the suppressive impacts of NaB on cell proliferation and invasion in OSCC. Moreover, the subcutaneous tumorigenesis experiment in nude mice validated the inhibitory impact of NaB on OSCC growth via the HDAC1/HSPB7 axis *in vivo*.

In conclusion, our mechanistic analysis revealed that HDAC1 inhibited HSPB7 expression through histone deacetylation. Further experiments on cellular and nude mice illustrated that NaB restricted OSCC cell proliferation and invasion *in vitro* as well as OSCC growth *in vivo* by facilitating HSPB7 expression via HDAC1 downregulation. These findings suggest that NaB may be a potential target for OSCC treatment and hopefully provide a new perspective for OSCC treatment. However, this study also suffers

from some limitations. No clinical tissues were collected and tested for HDAC1 and HSPB7 expression, and no clinical trials were performed. Therefore, future research is warranted for current topics.

Acknowledgments: This research was funded by the grant from Science and Technology Project of Jinchang City (Grant No. 2020BDD3NK).

References

- [1] CHAI AWY, LIM KP, CHEONG SC. Translational genomics and recent advances in oral squamous cell carcinoma. *Semin Cancer Biol* 2020; 61: 71–83. <https://doi.org/10.1016/j.semincancer.2019.09.011>
- [2] NADERI A. SRARP and HSPB7 are epigenetically regulated gene pairs that function as tumor suppressors and predict clinical outcome in malignancies. *Mol Oncol* 2018; 12: 724–755. <https://doi.org/10.1002/1878-0261.12195>
- [3] TANDON P, DADHICH A, SALUJA H, BAWANE S, SACHDEVA S. The prevalence of squamous cell carcinoma in different sites of oral cavity at our Rural Health Care Centre in Loni, Maharashtra – a retrospective 10-year study. *Contemp Oncol (Pozn)* 2017; 21: 178–183. <https://doi.org/10.5114/wo.2017.68628>

- [4] YANG Z, LIANG X, FU Y, LIU Y, ZHENG L et al. Identification of AUNIP as a candidate diagnostic and prognostic biomarker for oral squamous cell carcinoma. *EBioMedicine* 2019; 47: 44–57. <https://doi.org/10.1016/j.ebiom.2019.08.013>
- [5] DIKSHIT R, GUPTA PC, RAMASUNDARAHETTIGE C, GAJALAKSHMI V, ALEKSANDROWICZ L et al. Cancer mortality in India: a nationally representative survey. *Lancet* 2012; 379: 1807–1816. [https://doi.org/10.1016/S0140-6736\(12\)60358-4](https://doi.org/10.1016/S0140-6736(12)60358-4)
- [6] HUANG GZ, WU QQ, ZHENG ZN, SHAO TR, LV XZ. Identification of Candidate Biomarkers and Analysis of Prognostic Values in Oral Squamous Cell Carcinoma. *Front Oncol* 2019; 9: 1054. <https://doi.org/10.3389/fonc.2019.01054>
- [7] ZHAO X, SUN S, ZENG X, CUI L. Expression profiles analysis identifies a novel three-mRNA signature to predict overall survival in oral squamous cell carcinoma. *Am J Cancer Res* 2018; 8: 450–461.
- [8] GHARAT SA, MOMIN M, BHAVSAR C. Oral Squamous Cell Carcinoma: Current Treatment Strategies and Nanotechnology-Based Approaches for Prevention and Therapy. *Crit Rev Ther Drug Carrier Syst* 2016; 33: 363–400. <https://doi.org/10.1615/CritRevTherDrugCarrierSyst.2016016272>
- [9] DAN H, LIU S, LIU J, LIU D, YIN F et al. RACK1 promotes cancer progression by increasing the M2/M1 macrophage ratio via the NF-kappaB pathway in oral squamous cell carcinoma. *Mol Oncol* 2020; 14: 795–807. <https://doi.org/10.1002/1878-0261.12644>
- [10] MIKI Y, MUKAE S, MURAKAMI M, ISHIKAWA Y, ISHII T et al. Butyrate inhibits oral cancer cell proliferation and regulates expression of secretory phospholipase A2-X and COX-2. *Anticancer Res* 2007; 27: 1493–1502.
- [11] MAGRIN GL, DI SUMMA F, STRAUSS FJ, PANAHIPOUR L, MILDNER M et al. Butyrate Decreases ICAM-1 Expression in Human Oral Squamous Cell Carcinoma Cells. *Int J Mol Sci* 2020; 21: <https://doi.org/10.3390/ijms21051679>
- [12] ZHOU Z, XU N, MATEI N, MCBRIDE DW, DING Y et al. Sodium butyrate attenuated neuronal apoptosis via GPR41/Gbetagamma/PI3K/Akt pathway after MCAO in rats. *J Cereb Blood Flow Metab* 2021; 41: 267–281. <https://doi.org/10.1177/0271678X20910533>
- [13] GILLENWATER A, ZOU CP, ZHONG M, LOTAN R. Effects of sodium butyrate on growth, differentiation, and apoptosis in head and neck squamous carcinoma cell lines. *Head Neck* 2000; 22: 247–256. [https://doi.org/10.1002/\(sici\)1097-0347\(200005\)22:3<247::aid-hed7>3.0.co;2-o](https://doi.org/10.1002/(sici)1097-0347(200005)22:3<247::aid-hed7>3.0.co;2-o)
- [14] CARNIELLI CM, MACEDO CCS, DE ROSSI T, GRANATO DC, RIVERA C et al. Combining discovery and targeted proteomics reveals a prognostic signature in oral cancer. *Nat Commun* 2018; 9: 3598. <https://doi.org/10.1038/s41467-018-05696-2>
- [15] GONG L, WANG WM, JI Y, WANG Y, LI DW. [Effects of sodium butyrate on proliferation of human oral squamous carcinoma cell line and expression of p27Kip1]. *Zhonghua Kou Qiang Yi Xue Za Zhi* 2010; 45: 619–622.
- [16] TASOULAS J, GIAGINIS C, PATSOURIS E, MANOLIS E, THEOCHARIS S. Histone deacetylase inhibitors in oral squamous cell carcinoma treatment. *Expert Opin Investig Drugs* 2015; 24: 69–78. <https://doi.org/10.1517/13543784.2014.952368>
- [17] KRISHNA A, SINGH V, SINGH S, KUMAR S, KUMAR V et al. Upregulated histone deacetylase 2 gene correlates with the progression of oral squamous cell carcinoma. *Cancer Biomark* 2020; 29: 543–552. <https://doi.org/10.3233/CBM-190729>
- [18] AHN MY, YOON JH. Histone deacetylase 8 as a novel therapeutic target in oral squamous cell carcinoma. *Oncol Rep* 2017; 37: 540–546. <https://doi.org/10.3892/or.2016.5280>
- [19] RASTOGI B, RAUT SK, PANDA NK, RATTAN V, RADO-TRA BD et al. Overexpression of HDAC9 promotes oral squamous cell carcinoma growth, regulates cell cycle progression, and inhibits apoptosis. *Mol Cell Biochem* 2016; 415: 183–196. <https://doi.org/10.1007/s11010-016-2690-5>
- [20] CITRARO R, LEO A, DE CARO C, NESCI V, GALLO CANTAFIO ME et al. Effects of Histone Deacetylase Inhibitors on the Development of Epilepsy and Psychiatric Comorbidity in WAG/Rij Rats. *Mol Neurobiol* 2020; 57: 408–421. <https://doi.org/10.1007/s12035-019-01712-8>
- [21] DAVIE JR. Inhibition of histone deacetylase activity by butyrate. *J Nutr* 2003; 133: 2485S–2493S. <https://doi.org/10.1093/jn/133.7.2485S>
- [22] LIN J, DENG Z, TANIKAWA C, SHUIN T, MIKI T et al. Downregulation of the tumor suppressor HSPB7, involved in the p53 pathway, in renal cell carcinoma by hypermethylation. *Int J Oncol* 2014; 44: 1490–1498. <https://doi.org/10.3892/ijo.2014.2314>
- [23] LU Y, KOU Y, GAO Y, YANG P, LIU S et al. Eldecalcitol inhibits the progression of oral cancer by suppressing the expression of GPx-1. *Oral Dis* 2021. <https://doi.org/10.1111/odi.14010>
- [24] SHENG H, OGAWA T, NIWANO Y, SASAKI K, TACHIBANA K. Effects of polyphenols on doxorubicin-induced oral keratinocyte cytotoxicity and anticancer potency against oral cancer cells. *J Oral Pathol Med* 2018; 47: 368–374. <https://doi.org/10.1111/jop.12685>
- [25] MOFFAT J, GRUENEBERG DA, YANG X, KIM SY, KLOEPFER AM et al. A lentiviral RNAi library for human and mouse genes applied to an arrayed viral high-content screen. *Cell* 2006; 124: 1283–1298. <https://doi.org/10.1016/j.cell.2006.01.040>
- [26] STEWART SA, DYKXHOORN DM, PALLISER D, MIZUNO H, YU EY et al. Lentivirus-delivered stable gene silencing by RNAi in primary cells. *RNA* 2003; 9: 493–501. <https://doi.org/10.1261/rna.2192803>
- [27] XIAO TT, LI X, FENG JL, LI Y. Combined effects of aspirin and vitamin D3 on two OSCC cell lines: a preliminary study. *Biotechnol Lett* 2018; 40: 551–559. <https://doi.org/10.1007/s10529-018-2508-5>
- [28] HE B, LIN X, TIAN F, YU W, QIAO B. MiR-133a-3p Inhibits Oral Squamous Cell Carcinoma (OSCC) Proliferation and Invasion by Suppressing COL1A1. *J Cell Biochem* 2018; 119: 338–346. <https://doi.org/10.1002/jcb.26182>
- [29] YAO Y, CHEN S, LU N, YIN Y, LIU Z. LncRNA JPX overexpressed in oral squamous cell carcinoma drives malignancy via miR-944/CDH2 axis. *Oral Dis* 2021; 27: 924–933. <https://doi.org/10.1111/odi.13626>
- [30] MA Y, HAN J, LUO X. FOXD1-AS1 upregulates FOXD1 to promote oral squamous cell carcinoma progression. *Oral Dis* 2021. <https://doi.org/10.1111/odi.14002>

- [31] QIU F, QIAO B, ZHANG N, FANG Z, FENG L et al. Blocking circ-SCMH1 (hsa_circ_0011946) suppresses acquired DDP resistance of oral squamous cell carcinoma (OSCC) cells both in vitro and in vivo by sponging miR-338-3p and regulating LIN28B. *Cancer Cell Int* 2021; 21: 412. <https://doi.org/10.1186/s12935-021-02110-8>
- [32] ZHAO Z, CHU W, ZHENG Y, WANG C, YANG Y et al. Cytoplasmic eIF6 promotes OSCC malignant behavior through AKT pathway. *Cell Commun Signal* 2021; 19: 121. <https://doi.org/10.1186/s12964-021-00800-4>
- [33] ARJUNAN P, MEGHIL MM, PI W, XU J, LANG L et al. Oral Pathobiont Activates Anti-Apoptotic Pathway, Promoting both Immune Suppression and Oncogenic Cell Proliferation. *Sci Rep* 2018; 8: 16607. <https://doi.org/10.1038/s41598-018-35126-8>
- [34] FANG Z, ZHAO J, XIE W, SUN Q, WANG H et al. LncRNA UCA1 promotes proliferation and cisplatin resistance of oral squamous cell carcinoma by suppressing miR-184 expression. *Cancer Med* 2017; 6: 2897–2908. <https://doi.org/10.1002/cam4.1253>
- [35] LIU Y, LI RH, REN G, JIANG J. Suppression of KIF22 Inhibits Cell Proliferation and Xenograft Tumor Growth in Tongue Squamous Cell Carcinoma. *Biomed Res Int* 2020; 2020: 6387545. <https://doi.org/10.1155/2020/6387545>
- [36] NAITO S, VON ESCHENBACH AC, GIAVAZZI R, FIDLER IJ. Growth and metastasis of tumor cells isolated from a human renal cell carcinoma implanted into different organs of nude mice. *Cancer Res* 1986; 46: 4109–4115.
- [37] LV Y, LU J, LIU X, MIAO S, MAO X et al. Histone deacetylase 1 regulates the malignancy of oral cancer cells via miR-154-5p/PCNA axis. *Biol Chem* 2020; 401: 1273–1281. <https://doi.org/10.1515/hsz-2020-0189>
- [38] BOTHA H, FARAH CS, KOO K, CIRILLO N, MCCULLOUGH M et al. The Role of Glucose Transporters in Oral Squamous Cell Carcinoma. *Biomolecules* 2021; 11: 1070. <https://doi.org/10.3390/biom11081070>
- [39] SHIN H, LEE YS, LEE YC. Sodium butyrate-induced DAPK-mediated apoptosis in human gastric cancer cells. *Oncol Rep* 2012; 27: 1111–1115. <https://doi.org/10.3892/or.2011.1585>
- [40] XIAO M, LIU YG, ZOU MC, ZOU F. Sodium butyrate induces apoptosis of human colon cancer cells by modulating ERK and sphingosine kinase 2. *Biomed Environ Sci* 2014; 27: 197–203. <https://doi.org/10.3967/bes2014.040>
- [41] YAMATOJI M, KASAMATSU A, KOUZU Y, KOIKE H, SAKAMOTO Y et al. Dermatopontin: a potential predictor for metastasis of human oral cancer. *Int J Cancer* 2012; 130: 2903–2911. <https://doi.org/10.1002/ijc.26328>
- [42] OHTA M, ABE A, OHNO F, HASEGAWA Y, TANAKA H et al. Positive and negative regulation of podoplanin expression by TGF-beta and histone deacetylase inhibitors in oral and pharyngeal squamous cell carcinoma cell lines. *Oral Oncol* 2013; 49: 20–26. <https://doi.org/10.1016/j.oraloncology.2012.06.017>
- [43] WANG A, ZENG R, HUANG H. Retinoic acid and sodium butyrate as cell cycle regulators in the treatment of oral squamous carcinoma cells. *Oncol Res* 2008; 17: 175–182. <https://doi.org/10.3727/096504008785114129>
- [44] THEOCHARIS S, KLIJANIENKO J, GIAGINIS C, RODRIGUEZ J, JOUFFROY T et al. Histone deacetylase-1 and -2 expression in mobile tongue squamous cell carcinoma: associations with clinicopathological parameters and patients survival. *J Oral Pathol Med* 2011; 40: 706–714. <https://doi.org/10.1111/j.1600-0714.2011.01031.x>
- [45] NOHATA N, HANAZAWA T, KINOSHITA T, INAMINE A, KIKKAWA N et al. Tumour-suppressive microRNA-874 contributes to cell proliferation through targeting of histone deacetylase 1 in head and neck squamous cell carcinoma. *Br J Cancer* 2013; 108: 1648–1658. <https://doi.org/10.1038/bjc.2013.122>
- [46] REID T, VALONE F, LIPERA W, IRWIN D, PAROLY W et al. Phase II trial of the histone deacetylase inhibitor pivaloyloxymethyl butyrate (Pivanex, AN-9) in advanced non-small cell lung cancer. *Lung Cancer* 2004; 45: 381–386. <https://doi.org/10.1016/j.lungcan.2004.03.002>
- [47] JIN C, SHUAI T, TANG Z. HSPB7 regulates osteogenic differentiation of human adipose derived stem cells via ERK signaling pathway. *Stem Cell Res Ther* 2020; 11: 450. <https://doi.org/10.1186/s13287-020-01965-4>